A Numerical Study of the Track Deflection of Supertyphoon Haitang (2005) Prior to its Landfall in Taiwan

Guo-Ji Jian[1] and Chun-Chieh Wu[2]
[1]Meteorological Forecast Center, Central Weather Bureau, Taipei, Taiwan
[2]Department of Atmospheric Sciences, National Taiwan University

1. Introduction

Landfalling typhoons pose a serious threat to life and property. During the landfall period, typhoon's inner core often displays highly asymmetric distribution of strong winds and deep convection. When the typhoon approaches a region with the complex terrain, the asymmetric structures may become more complicated and result in various types of track deflection and wind and rainfall distributions (Wu and Kuo 1999). A detailed investigation of such track deflection is of great importance to hazard mitigation since the most severe damage appears to be highly related to the typhoon's landfall location and the landfall time. For instance, Supertyphoon Haitang (2005) moved steadily northwestward toward Taiwan with some erratic track, i.e., turning sharply southward and executing a cyclonic loop about 50 – 60 km east of Taiwan, before finally making landfall on 18 July (Fig. 1). It took Haitang about 24 h to cross the island, resulting in 12 fatalities, as well as property damage of at least US $150 millions in the Taiwan area. In this study, a series of numerical simulations are performed to examine the physical processes responsible for the significant track deflection of Haitang prior to its landfall in Taiwan. All experiments are simulated with the highest horizontal resolution of 4 km using the Advanced Research WRF (WRF-ARW) modeling system, version 2.0.3 (Skamarock et al. 2005). All the 72-h model simulations begin at 0000 UTC 17 July 2005.

2. Model description and experiment design

a. Model configuration and, initial conditions

The WRF-ARW system solves the compressible, nonhydrostatic flux-form Euler equations in a terrain-following hydrostatic- pressure vertical coordinate (η coordinate). The model domains are a stationary 4 km mesh (121x121) nested within a 12 km (191×191) mesh using a two-way interactive method. Both domains extend vertically to 100 hPa and are resolved by 31 η levels, with 8 levels in the lowest 1 km. The model topography (see Fig. 1 for the Taiwan terrain in the 4 km domain) is interpolated from terrain data with 30" resolution. Information on land use is obtained from U.S. Geological Survey (USGS) with the same resolution as for the topography use.

The physics of the model includes the WRF Single-Moment five-class microphysics (Hong et al. 2004), Yosei University planetary boundary layer (PBL) scheme (Hong et al. 2003), five-layer soil model (Chen and Dudhia 2003), Rapid Radiative Transfer Model longwave radiation (Mlawer et al. 1997), and Dudhia shortwave radiation scheme (Dudhia 1989). The modified version of Kain-Fritsch convective parameterization (Kain 2004) is also used in outer domain. The model initial conditions are taken from the operational CWB Nonhydrostatic Forecasting System (NFS) analyses. These data are available every 12 h on a 15 km × 15 km grid. A proper typhoon bogus scheme (NCAR-AFWA scheme; Davis and Low-Nam 2001) is emplyed in this study to enhance the description of the initial model vortex. The lateral boundary conditions are obtained from the operational NFS forecast at 6-h intervals

b. Design of numerical experiments

To explore the dynamics involved in the significant track deflection before Haitang's landfall in Taiwan, a series of numerical experiments are designed as follows. All 72-h integration experiments are initialized at 0000 UTC 17 July 2005, i.e., about 24 h before the occurrence of the looping motion..

- CTRL: this control experiment includes full Taiwan terrain and applies the NCAR-AFWA bogus scheme (Davis and Low-Nam 2001) to implant an initial vortex into the operational CWB NFS analysis. In CTRL, the maximum tangential wind speed, the radius of maximum wind (RMW) and the exponential parameter (α), which specifies the horizontal wind profile outside the RMW of the Rankine vortex are set to 53 ms^{-1}, 50 km, and 0.6, respectively.
- H07, H04, and H01: these experiments are the same as in CTRL, except that the numerical simulations are carried out while the terrain height of Taiwan at each grid point is reduced to 0.7, 0.4, and 0.1, respectively, relative to that in CTRL.

- FLAT: this experiment is the same as in CTRL, except that the Taiwan terrain is removed and set to 1 m in elevation, while the land–sea attributes remain unchanged.
- NT: this experiment is the same as in CTRL, except that the Taiwan terrain is completely removed and values of land state variables (such as landuse, soil types,... etc.) in Taiwan are switched to the ocean conditions.
- A35 and A47: these experiments are the same as in CTRL, except that the value of α in the bogus vortex is set to 0.35 and 0.47, respectively.
- NT_A35 and NT_A47: these experiments are the same as in NT, except that the value of α in the bogus vortex is set to 0.35 and 0.47, respectively.

Comparisons from the above numerical experiments are expected to provide helpful information to improve our understanding of the factors that influence Haitang's track near Taiwan, such as the role of the terrain height of Taiwan, and the impact of the vortex structure, i.e., with different values of α in the initial vortex.

3. Results

3.1 Control experiment (CTRL)

In the control experiment with full Taiwan terrain, the simulated track is remarkably consistent with Haitang's best track during the 72-h integration, especially regarding the looping motion off the east coast of Taiwan and the landfall location to the north of Hua-Lien, Taiwan (Fig. 2). Note that the looping motion disappears in the experiment NT, suggesting that the presence of the Taiwan terrain plays a significant role in deflecting the track of Haitang, especially during the pre-landfall period.

Based on the analysis of the above simulation results, a conceptual model of Haitang's interaction with the Taiwan terrain is shown schematically in Fig. 3. As Haitang is located about 60 km east of Taiwan, to maintain the fluid continuity, the low-level flow passing through the western side of storm center (shown as the area A2 in Fig. 3) accelerates since the air parcels are originated from a relatively wider area (shown as the area A1 in Fig. 3). This physical process is commonly referred to as the channeling effect and potentially important while the inner core circulation of the approaching typhoon squeezed due to the presence of the Taiwan terrain (e.g., Lin et al., 2005). Through the channeling effect, a low-level northerly jet forms and intensifies in the western quadrant of the eyewall. This low-level northerly jet eventually becomes the strongest winds of the storm in CTRL. A field of asymmetric winds arises within the inner core afterwards, and induces a northerly ventilation flow that forces the storm to turn sharply southward (Fig. 4). During this stage, the movement of the simulated storm most closely matches with the ventilation wind vectors at the 700- and 600-hPa pressure levels. These results reveal that the strongest winds of the storm located at the region of the low-level northerly jet (western side of the eyewall) is a crucial feature in determining the sharply southward turn during the period of Haitang's looping motion.

3.2 Sensitivity experiments

Sensitivity experiments in which the Taiwan terrain is artificially modified indicate that the decrease of the terrain height of Taiwan reduces the response of the storm's track deflection as it approaches the terrain barrier. Even with the lower terrain (e.g., experiment H04), the simulated storm also exhibits a looping path just before landfall as long as the low-level northerly jet coincides with the strongest winds of the eyewall (as in H07 and H04). However, when the terrain height is drastically reduced (e.g., experiments H01 and FLAT), the looping motion of Haitang does not occur any more since the channeling of winds in the western eyewall is not strong enough to establish the northerly ventilation flow. For instance, in H01, the strongest winds of the storm are generally located in the north-northeastern and northern quadrants. These wind asymmetries tend to correspond to an easterly ventilation flow, which tends to steer the simulated storm westward. The above results suggest that the presence of the high terrain in Taiwan results in the strong low-level northerly jet on the western side of Haitang's eyewall. Once the strongest winds in the eyewall are collocated with this northerly jet, the storm would experience some southward drift and result in a cyclonic loop just prior to the landfall.

The approaching storm is stronger and larger when using a smaller value of exponential parameter (α) in the initial vortex. The comparison between experiments applying different value of α exposes the effects of winds distribution (especially in storm's inner core) on the track changes of Haitang. As an example, the storm in A35 (α=0.35) tends to move faster and therefore with the earlier landfalling time than that of CTRL (α=0.60). It is worth noting that the strength of the low-level northerly jet (~ 55 – 56 m s^{-1}) in A35 is quite similar to that of CTRL, implicating that the strong channeling effect occurs in both simulations as the storm approaches Taiwan. However, the storm in A35 follows a straight track without making a loop during its pre-landfall period. The differences are mainly caused by two factors. First, the storm in A35 is a larger, more intense, and rapidly moving vortex and therefore would be more likely to move across the Taiwan terrain with less time to experience the southward deflection. Second, although the low-level northerly jet is also pronounced in the western portion of the eyewall, the strongest winds associated with the storm of A35, however, are located in the eastern quadrant of the eyewall [see Fig. 5 and $(V_{max})_{east}$ in Fig. 3]. The winds distribution in the storm of A35 does not have an average southward steering flow as that in CTRL. The above results demonstrate that the second factor is especially important for determining the sharp track deflection associated with a typhoon (e.g., Supertyphoon Haitang) near Taiwan.

References

Chen, S.-H., and J. Dudhia cited. , 2003: Annual report: WRF physics. Air Force Weather Agency, 38 pp. [Available online at http://www.mmm.ucar.edu/wrf /users/docs/wrf-phy.html.].

Davis, C. A., and S. Low-Nam, 2001: The NCAR-AFWA tropical cyclone bogussing scheme. *NCAR Technical Note,* 13pp. [Available online at http://www.mmm. ucar.edu/mm5/mm5v3/tc-report.pdf.]

Dudhia, J., 1989: Numerical study of convection observed during the winter monsoon experiment using a mesoscale two-dimensional model. *J. Atmos. Sci.,* **46**, 3077–3107.

Hong, S.-Y., J. Dudhia, and S.-H. Chen, 2004: A Revised Approach to Ice Microphysical Processes for the Bulk Parameterization of Clouds and Precipitation, Mon. Wea. Rev., **132**, 103–120.

———, J. Dudhia, and Y. Noh, 2003: A new vertical diffusion package with explicit treatment of the entrainment processes. *Proc. Int. Workshop on NWP Models for Heavy Precipitation in Asia and Pacific Areas*, Tokyo, Japan, Japan Meteorological Agency, 52-58.

Kain, J. S., 2004: The Kain–Fritsch convective parameterization: An update. *J. Appl. Meteor.,* **43**, 170–181.

Lin, Y.–L., S.–Y. Chen, C. M. Hill, and C.–Y. Huang, 2005: Control parameters for the influence of a mesoscale mountain range on cyclone track continuity and deflection. *J. Atmos. Sci.*, **62,** 1849-1866.

Mlawer, E. J., S. J. Taubman, P. D. Brown, M. J. Iacono, and S. A. Clough, 1997: Radiative transfer for inhomogeneous atmospheres: RRTM, a validated correlated-*k* model for the long-wave. *J. Geophys. Res.,* **102**, 16663–16682.

Skamarock, W. C., J. B. Klemp, J. Dudhia, D. O. Gill, D. M. Barker, W. Wang and J. G. Powers, 2005: A Description of the Advanced Research WRF Version 2. NCAR Technical Note, NCAR/TN-468+STR, 88pp.

Wu, C. –C., and Y. –H. Kuo, 1999: Typhoons affecting Taiwan: Current understanding and future challenges. *Bull. Amer. Meteor. Soc.*, **80,** 67-80.

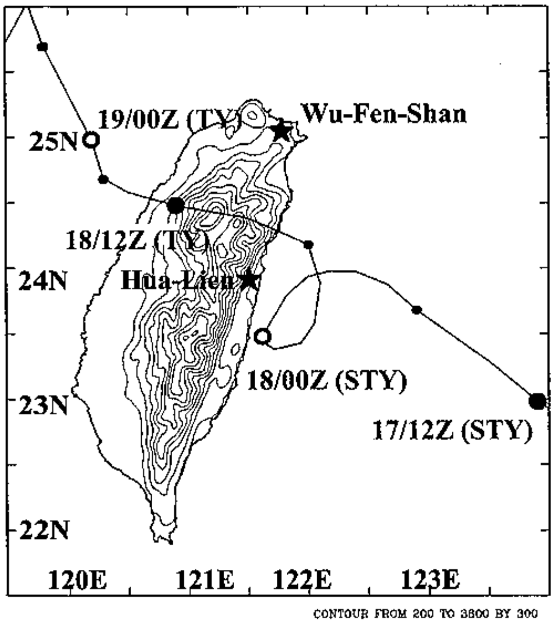

Fig. 1. Supertyphoon Haitang made a slow cyclonic loop off the eastern coast of Taiwan. Small bold circles are the best tracks at 0600 UTC and 1800 UTC. The two star symbols show the locations of Wu-Fen-Shan and Hua-Lien Doppler radar stations.

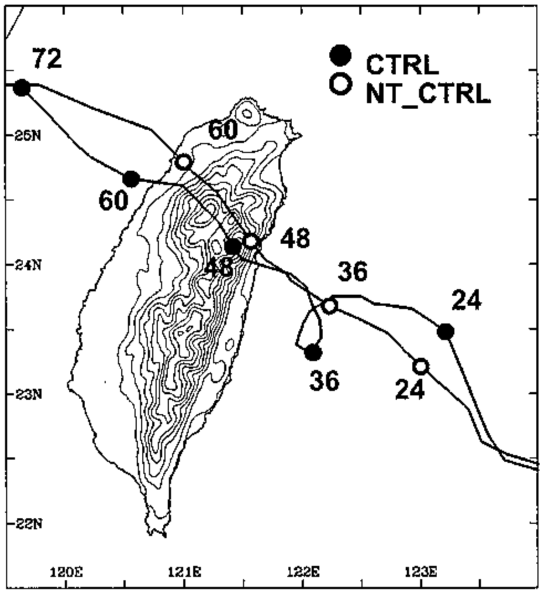

Fig. 2. The simulated tracks comparison of CTRL (marked by bold circles) and NT (marked by open circles). The Taiwan terrain (thin lines) used in experiment CTRL is also drawn from 200 m high with a contour interval of 300 m.

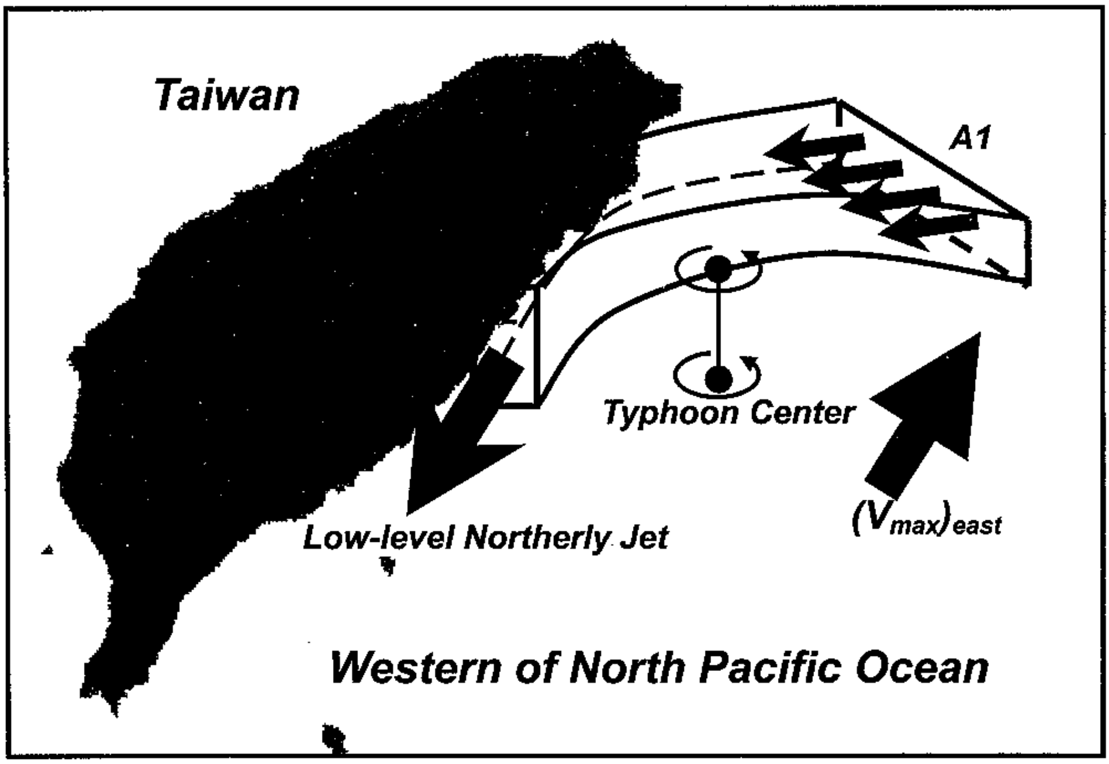

Fig. 3. Schematic diagram summarizing the formation of low-level northerly jet as Supertyphoon Haitang (2005) approached Taiwan. Air parcels passing from a wider vertical cross section (A1) to a narrower vertical cross section (A2) (i.e., the channeling effect) is a major factor for the acceleration of the flow. The storm would experience some southward drift before landfall if the strength of the low-level northerly jet is greater than the maximum wind in the eastern quadrant of the eyewall.

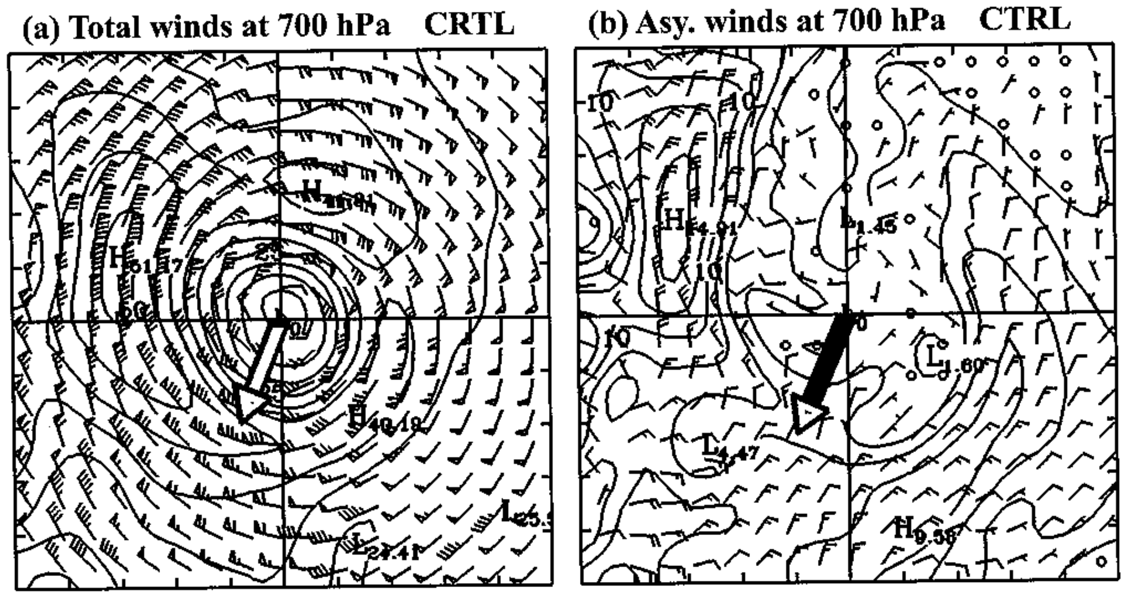

Fig. 4. (a) Simulated total wind fields (left; contour interval of 5 m s^{-1}) and (b) the asymmetric wind fields (right; contour interval of 2 m s^{-1}) in CTRL at the 33-h model simulation. The open arrow in (a) indicates the vortex motion (3.3 m s^{-1}). The bold arrow in (b) shows the average asymmetric flow in a 100-km radius from the vortex center at 700 hPa (4.0 m s^{-1}). The domain shown in each panel is 200 km by 200 km.

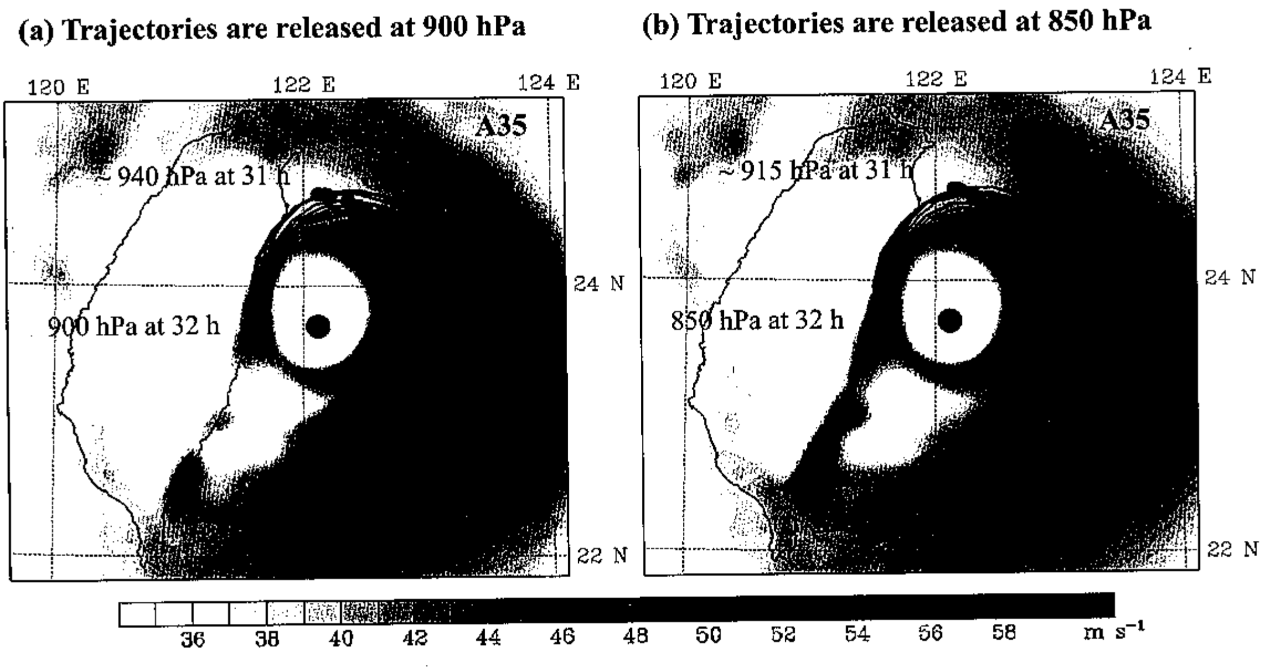

Fig. 5. Backward trajectories based on the WRF-ARW-simulated winds from experiment A35. Parcels are released from (a) 900 hPa and (b) 850 hPa pressure levels at 32 h and calculated backward for 3 h. Horizontal wind speeds are shaded for values greater than 36 m s^{-1}.(as shown in the gray scale).